Applied Catalysis B: Environmental 99 (2010) 96–102

Contents lists available at ScienceDirect

Applied Catalysis B: Environmental

journal homepage: www.elsevier.com/locate/apcatb

Highly ordered TiO_2 nanotube arrays and photoelectrocatalytic oxidation of aromatic amine

Juliano Carvalho Cardoso, Thiago Mescoloto Lizier, Maria Valnice Boldrin Zanoni*

Departamento de Química Analítica, Instituto de Química, University Estadual Paulista, UNESP, Av. Prof. Francisco degni, s/n, C. P. 355 14801-970 Araraquara, SP, Brazil

ARTICLE INFO

Article history:
Received 18 December 2009
Received in revised form 31 May 2010
Accepted 7 June 2010
Available online 11 June 2010

Keywords:
Aromatic amines
Photoelectrocatalysis
TiO_2 nanotubes array electrodes
4,4′-Oxydianiline
Amine removal

ABSTRACT

Self-organized Ti/TiO_2 nanotubular array electrodes may be achieved by simple electrochemical anodization of Ti foil in NH_4F/glycerol water solution. The photocurrent on nanotubular layers is remarkably improved in relation to that obtained on comparable nanoporous TiO_2 films created by a sol gel process. The anatase form is priori in the highly ordered TiO_2 annealed at 450 °C which improves its photoactivity. Both electrodes promote complete degradation of the investigated aromatic amine ODAN (4,4′-oxydianiline) after 120 min of photoeletrocatalytic oxidation with potential of 1.5 V and UV irradiation. But, the ODAN mineralization is about 50% more efficient on nanotubular electrodes. The best experimental conditions were found to be pH 2.0 and 0.1 mol L^{-1} Na_2SO_4 when the photoelectrode was biased at +1.5 V (vs. SCE). Complete mineralization of the aromatic amine content (100% TOC reduction) was achieved after 2 h. Effects of other electrolytes, pH, amine concentration and applied potentials also have been investigated and are discussed.

1. Introduction

Aromatic amines can enter the aqueous environment via azo dyes and nitroaromatic compounds reductions [1–3] and have been identified as potential carcinogens [4]. These compounds are important class of anthropogenic chemicals [5] used in the preparation of a large number of synthetic organic compounds. Since they have been deemed as high priority pollutants, their presence in the environment must be carefully monitored and suitable remediation treatments are required for water, wastewater, or soil to obtain concentration levels compatible with the limits admitted by the regulation at 30 ppm.

In order to eliminate or reduce the serious health risks associated with the presence of aromatics amines in the environment, in particular in the aquatic phase, different processes have been suggested and developed for the treatment of water and wastewater containing trace amounts of these toxic chemicals [6]. The most proposed methods for the removal of aromatic amines are based on biodegradation [6–8], photo-fenton process [9] and photocatalysis on TiO_2 powder [10–14]. But, all of the proposed methods report low efficiency of the degradation aromatic amines as well as the formation of toxic sub-products as: phenol, 2-aminophenol, N,N-dimethylaniniline, nitrobenzene, 4-aminophenol and others due to partial degradation of aromatic amines.

4,4′-Oxydianiline (ODAN) is widely used in the production of epoxy resins, polyimides, and poly(ester) imides resins which are commonly used in the manufacture of adhesives, insulating varnishes, coated fabrics, flame retardant fibers, oil sealants, insulation for cables and printed circuits and composites for aerospace vehicles, heat resistant wire enamels and others. In addition, it is an intermediate in the synthesis of dyes and is used in dyeing processes involved in leather manufacturing. ODAN is slightly toxic via oral route, but has indicated positive response for mutagenic test in salmonella typhymurium and in vitro chromosome aberration and induced carcinogenic evidence in experimental animals. Although, this compound is condemned by IARC and is released in waste streams from its production and use, there is no study in the literature dealing with the complete removal of ODAN from wastewaters.

Photoreactive materials as titania (TiO_2) have received much attention as an excellent material for photodegradation of organic pollutants in water [15,16]. An attractive strategy to increase the photocatalytic efficiency consists of introducing a reverse bias potential to the anode coated by the photocatalyst. Examples of such photoelectrocatalytic oxidation of organic pollutants are available [14–20]. The main techniques used to prepare Ti/TiO_2 coating are based on sol–gel process, precipitation–peptization, hydrothermal synthesis, electrochemical methods and template models [21–28]. But, it has been confirmed that the architecture of titania can greatly influence its physicochemical properties [18,19]. Alternatively, highly ordered nanotubular arrays of TiO_2 show a porous surface, quite large surface area and oriented electron trans-

* Corresponding author.
E-mail address: boldrinv@iq.unesp.br (M.V.B. Zanoni).

0926-3373/$ – see front matter © 2010 Elsevier B.V. All rights reserved.
doi:10.1016/j.apcatb.2010.06.005

port, which affects the charge separation efficiency [27–36]. These conditions make TiO_2 nanotubular film an ideal material for photoelectrocatalysis, but in spite of its real advantage, few studies have been conducted on the application of this new technology for the remediation of aromatic amines.

Thus, the objective of this research was to construct nanotubular Ti/TiO_2 array electrodes by an anodization process and to assess its photoelectrooxidation efficiency with respect to the degradation of aromatic amine 4,4′-oxydianiline in aqueous solution. Their performance was compared with Ti/TiO_2 photoanodes prepared by the sol–gel method. The aromatic amine degradation kinetics parameters have been evaluated through analytical methods as UV–Vis spectrophotometry and high performance liquid chromatography with diode array detector and total organic carbon (TOC) removal to assess the effectiveness of the photoelectrocatalytic method with the aim to find an alternative method for wastewater purification containing this harmful pollutant.

2. Materials and methods

2.1. Preparation of TiO_2 nanotubes by electrochemical anodization

The titanium foils (99.95%, Alfa Aesar), 0.25 mm thick were polished to a mirror quality smooth finish using silicon carbide sandpaper of successively finer roughness (220, 320, 400, 800, 1200, and 1500 grit) and degreased by successively sonication for 15 min in isopropanol, acetone and finally ultrapure water. They were then dried under a flowing N_2 stream and used immediately. Highly ordered TiO_2 nanotubular arrays were prepared by a potentiostatic anodization in a two-electrode electrochemical cell. A titanium foil with a size of 5 cm × 5 cm was used as a working electrode, and a platinum foil with a size of 2 cm × 2 cm served as a counter electrode. The interval between working electrode and counter electrode was about 2 cm. The voltage was applied by a DC power supply (model MQ of Microquímica, Brazil). The TiO_2 nanotube array was formed by anodizing the Ti foil in 150 mL of organic electrolyte, which showed a dependence on the anodization time. The present organic electrolyte was 0.25% ammonium fluoride (97.0%, Fisher) in glycerol (98.5%, Fisher) containing 10% volume Milli-Q water. The grown porous layers were annealed at 450 °C for 30 min in a furnace (model 650-14 Isotemp Programmable Muffle Furnace, Fisher Scientific) and were allowed to cool gradually back to the ambient condition.

The crystallinity of the TiO_2 nanotubular arrays was studied using a Hitachi S-4800 scanning electron microscope. X-ray diffraction (XRD) patterns were measured on a Rigaku RINT 1500 X-ray diffraction meter using Cu KR radiation in the range of 20–60° and the structures and morphologies were characterized using JEOL JSM-6300 field emission scanning electron microscope (FEG-SEM) of LME-LNLS, Sincroton, Campinas-SP.

2.2. Preparation of TiO_2 nanoporous by sol gel method

Titanium (IV) isopropoxide (Aldrich) was used as a precursor for preparing TiO_2 colloidal suspensions. Typically, 20 mL of titanium isopropoxide was added to a nitric acid solution keeping the ratio of $Ti/H^+/H_2O$ at 1/1.5/200. The resulting precipitate was continuously stirred until completely peptized to a stable colloidal suspension. This suspension was dialyzed against ultrapure water (Milli-Q Millipore) to a pH of 3.5 using a Micropore 3500 MW membrane. Thin-film photoelectrodes were dip-coated onto a titanium-foil backed contact (0.05 or 0.5 mm thick, Goodfellow Cambridge Ltd.) after heating the Ti foils to 450 °C. A sequence of dipping, drying and firing at 450 °C for 3 h was used after each coating (four repetitions).

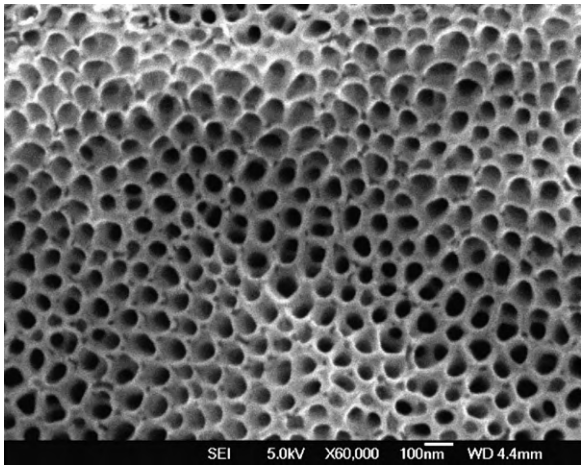

Fig. 1. FEG-SEM images of titania nanotubes prepared by anodization in 10 wt% water + 0.5 wt% NH_4F in glycerol at 30 V for 50 h.

2.3. Degradation experiments

The photoelectrocatalytic (PEC) experiments were performed in a 250 mL cylindrical glass reactor, with an ultraviolet (UV) irradiation (a 150 W high pressure mercury lamp from Oriel with a maximum wavelength of 365 nm), vertically inserted in a central quartz glass bulb. The counter electrode was a Pt gauze counter electrode and a saturated Ag/AgCl was used as reference electrode immerse in Luggin capillary. The working electrode was the TiO_2 nanotube array or TiO_2 nanoparticle on titanium foil of same geometric area, prepared as previously demonstrated elsewhere [34,26].

2.4. Spectroscopy, chromatographic and organic carbon analysis

Absorption spectra in the ultraviolet and visible range were recorded with a Hewlett-Packard spectrophotometer, model HP 8452A in a 10 mm quartz cell. Total organic carbon analyzer (TOC-V_{CPN}, Shimadzu, Japan) was employed for mineralization degree analysis of ODAN solution. Prior to injection into the TOC analyzer, the samples were filtrated with 0.45 μm Millipore filter to remove any particles. A high performance liquid chromatograph Model Shimadzu 10 AVP coupled with a diode array detector was used to separate the products and intermediates generates. A column separation C-18 (4.6 mm × 250 mm, 5 mm) and mobile phase methanol/phosphate buffer (50:50 (v/v)) with a flow of 1.0 mL min^{-1} were used. The signals from the detector were analyzed by integration of the area. The aromatic amine peak was monitored in 244 nm. The procedures were performed in triplicate for each sample.

3. Results and discussion

3.1. Characteristics of Ti/TiO_2 nanotubular arrays

The first set of experiments was done to monitor the growth of nanotubes. The anodizing solution used for the experiments consisted of 0.25% NH_4F, 10% water in glycerol as electrolyte. The experiments were carried out at room temperature (25 °C), with an anodization voltage at 30 V for 50 h. The growth of the TiO_2 nanotubes was monitored by taking FEG-SEM images.

Fig. 1 shows FEG-SEM images of TiO_2 layers formed by this anodic treatment. It is clear that the TiO_2 layer consists of nanotubular arrays with uniform tube diameter of 100 nm and wall thickness of 10 nm. The formation of nanotubular arrays was the

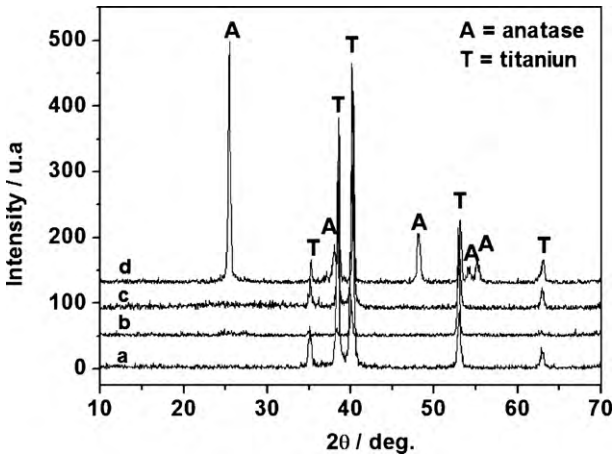

Fig. 2. X-ray diffraction patterns of titanium foil (a); TiO_2 nanolayers method sol–gel (b); TiO_2 nanotube arrays without annealed (c) and TiO_2 nanotube arrays annealed at 450 °C for 30 min (d).

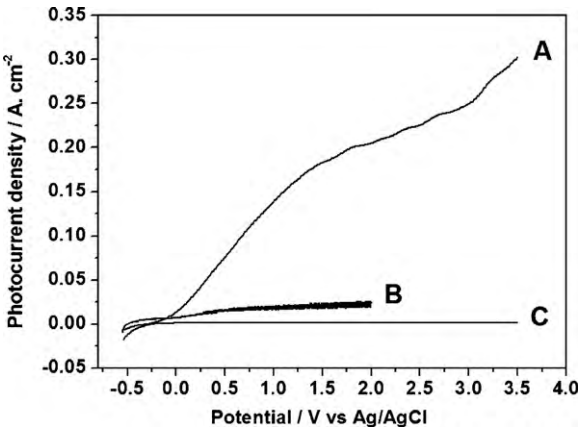

Fig. 3. Linear sweep voltammogram curves of (a) Ti/TiO_2 nanotubes arrays electrode (b) Ti/TiO_2 nanoporous electrode (c) Ti/TiO_2 nanotubular array electrode in 0.1 M Na_2SO_4 solution pH 6.0 in the dark or UV illumination.

result of a competition between electrochemical oxidation of titanium at the metal surface and chemical dissolution of the formed TiO_2 layer by fluorides in an electrolyte [28,37]. In order to make the competition available, glycerol was used as high viscous neutral electrolytes, adopted to control the steady process [38]. As it is well known, diffusion constant D is proportional to $1/\eta$ in terms of the Stokes–Einstein relation, where η is the solution viscosity. Moreover, the chemical reaction process of forming TiO_2 nanotube arrays has been expressed as Eqs. (1) and (2) where Eq. (1) represents TiO_2 formation by anodic oxidation and Eq. (2) represents TiO_2 dissolution by chemical process, respectively [39,40].

$$Ti + O_2 \rightarrow TiO_2 \quad (1)$$

$$TiO_2 + 6F^- + 4H^+ \rightarrow [TiF_6]^{2-} + 2H_2O \quad (2)$$

Hence, it can be concluded that high viscous solutions have low ion diffusion and may make the pore bottom retain a relatively high H^+ concentration produced by Eq. (1), which promotes the chemical drilling at the bottom of the nanotubes based on Eq. (2). On the other hand, neutral electrolytes are adopted to fabricate TiO_2 nanotubular arrays because they, as mild anodic oxidizing reactants, essentially suppress the chemical dissolution of the TiO_2 nanotube wall in comparison with acidic solutions [37]. As result, it is possible to obtain a self-assembly of nanotubular TiO_2 arrays films on the Ti surface using a simple step of anodization and subsequent annealing.

3.2. XRD analysis

Fig. 2 shows the XRD patterns of the TiO_2 nanotube arrays and TiO_2 nanoparticles prepared as listed in the reference [40], after being annealed at 450 °C under ambient air for 30 min. For reference, the pattern of pure titanium metal is also listed. The diffraction peaks at about 2θ: 25.5°, 37.3°, 38.1°, 48.2°, 54.2°, and 55.2° can be indexed to the (1 0 1), (1 0 3), (0 0 4), (2 0 0), (1 0 5), and (2 1 1) crystal faces of anatase TiO_2. Anatase form is preponderant in the composition of TiO_2 nanotubular electrodes electrochemically prepared. This is an advantage since in the field of photoelectrochemistry, anatase form has higher activity than other forms because it preserves more OH^- surface active sites, which is the photoactive form [34,39–41].

Taking into account that the photoactivity is dependent on the crystallinity of TiO_2, crystallite size, large surface area and porosity it was investigated the performance of the constructed TiO_2 nanotube arrays as photoanode in 0.1 M Na_2SO_4 under UV irradiation. The photocurrent density vs. applied potential with and without UV irradiation are shown in Fig. 3. The observed dark current for both samples was found to be negligible, see Fig. 3, curve C, but the short-circuit photocurrent density of the nanotube array (Fig. 3A) is more than six times the value obtained for nanoporous electrode obtained by sol–gel method (Fig. 3B) [42]. The enhanced photoresponse of the sample anodized in glycerol and NH_4F, may be due to the distinct tube structure. It is possible to observe that longer TiO_2 nanotubes are more efficient at light trapping which in turn results in enhanced photoconversion efficiency. Furthermore, the nanotube length within the array has seen results in a larger effective surface area thus enabling diffusive transport of photogenerated holes to $OH^\bullet$ generation due water oxidation. Thus, the marked increases in current on nanotubular photoelectrode indicates that the high efficiency is a synergic effect of large semiconductor/electrolyte interface due higher surface areas, minority carriers generated within a distance from the surface equal to the sum of the width of the depletion layer and the diffusion length escape recombination and smaller recombination of e^-/h^+ [43,44].

3.3. Degradation of ODAN on Ti/TiO_2 nanotubes electrodes

In order check the importance of bias potential in the photoelectrocatalytic process some experiments were conducted monitoring degradation of 1.0×10^{-4} mol L^{-1} ODAN in 0.1 mol L^{-1} Na_2SO_4 pH 6.0, under UV irradiation. Fig. 4 shows the potential effect ranged between +0.5 and +2.0 V on degradation followed at 244 nm (Fig. 4A) and monitored by TOC removal (Fig. 4B). Concentration was determined by monitoring the absorbance of amine at λ = 244 nm, from the UV–Visible absorption spectra as a function of time (shown in Fig. 5) and also by HPLC with diode array (Fig. 6).

The chromatographic behavior of ODAN using the best experimental condition as defined in the experimental shows a well defined peak with retention time of 4.5 min. After 60 min of analysis, the total reduction of original peak ODAN and formation of three intermediary compounds were observed. The complete reduction these compounds are observed after three hours of treatment.

As calculated from onset potential measurements, the flat-band potential obtained for the TiO_2 nanotubular array electrode in 0.1 mol L^{-1} Na_2SO_4 media is about −0.15 V. Therefore, all the applied potentials employed in this study are positive of the flat-band potential. So, there is always a potential gradient over the titania film, resulting in an electric field, which keeps photogenerated charges apart. These results suggest that adsorption of the ODAN is enhanced and/or the generation and separation of electron–hole pairs are accelerated under higher voltage condi-

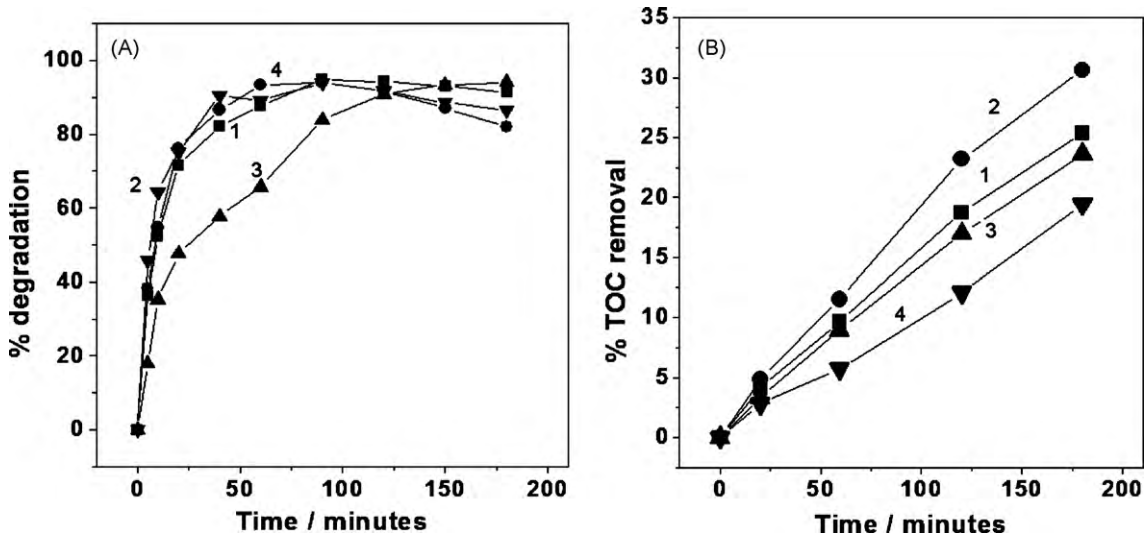

Fig. 4. PEC degradation of ODAN as affected by bias potential (initial concentration of ODAN 1.0×10^{-4} mol L^{-1}, bias potential 1.5 V, pH 6.0 and concentration of Na_2SO_4 0.1 mol L^{-1}) where: (1) +2.0; (2) +1.5; (3) +1.0 and (4) +0.5 V (vs. Ag/AgCl).

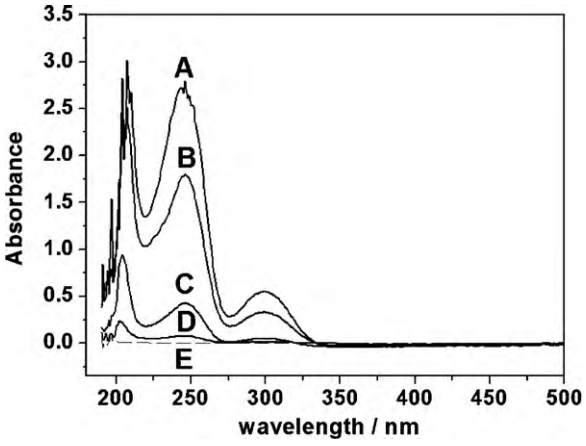

Fig. 5. UV–Vis absorption spectra for 1.0×10^{-4} mol L^{-1} ODAN in: 0.1 mol L^{-1} Na_2SO_4 at pH 6.0 before (curve (A)) and after 10 min of photoelectrocatalytic degradation (curve (B)); 20 min (curve (C)); 30 min (curve (D)) curve (E) blank on the TiO_2 nanotubular array electrode biased at +1.5 V (vs. Ag/AgCl).

tions. As a result, the rate of recombination decreases, so as to increase the photocurrent as a function of the applied potential. Accordingly, more of the active oxidizing radical species are thereby formed at higher potential, which promotes faster aromatic amine decomposition. In all further experiments +1.5 V was chosen as best potential for investigating the degradation of the ODAN.

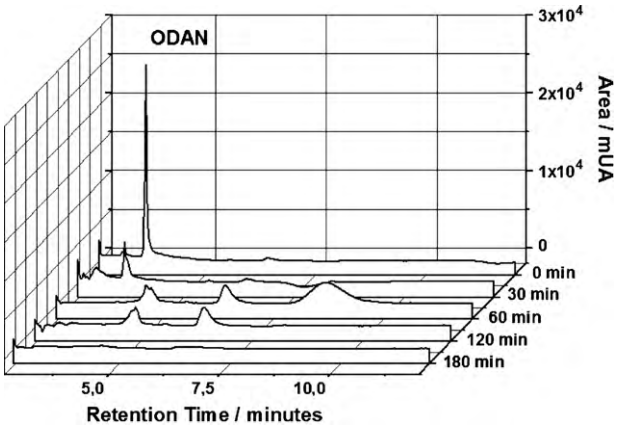

Fig. 6. Diode array chromatograms of ODAN treated solution for 0–180 min.

3.4. Effect of ODAN concentration

In order to obtain the best performance of the nanotube Ti/TiO_2 on the photoelectrocatalytic decomposition ODAN, its efficiency was investigated by testing solutions 1.0×10^{-6} to 1.0×10^{-4} mol L^{-1} concentrations of ODAN in 0.1 mol L^{-1} Na_2SO_4. The influence of initial concentration on the percentage of ODAN oxidation was followed by UV–Visible absorption spectra at 244 nm (Fig. 7A) and TOC removal (Fig. 7B). The results obtained monitoring the absorbance at 244 nm indicates that for a process operating under UV light and 1.5 V there is complete removal of ODAN after 180 min of treatment. But, although expressive TOC removal is obtained at concentration lower than 5.0×10^{-6} mol L^{-1}, the degradation percentage decreases successively for higher concentrations and presents negligible effect for ODAN mineralization at 1×10^{-4} mol L^{-1}. These findings indicate that the light intensity reaching the TiO_2 thin-film surface is reduced due to the lower transparency of the solution or the quantity of intermediates increased as well, competing through side reactions with the amine decomposition. These results suggest that photoelectrocatalysis is likely a very efficient method to treat amine wastewater under diluted solution conditions or the method could be coupled with another preceding treatment to reduce the discharge of organic contaminants.

3.5. Effect of supporting electrolyte and pH

The influence of the supporting electrolyte on the degradation of 5.0×10^{-6} mol L^{-1} ODAN was investigated through experiments conducted with in 0.1 mol L^{-1} of NaCl, $NaNO_3$ and Na_2SO_4. The Fig. 8 shows the percentage of degradation (A) and TOC removal (B) during 180 min of treatment in each supporting electrolyte. Although, there is 100% of degradation of ODAN in all observed supporting electrolytes (Fig. 8A), the results involving sodium sulfate promotes largest efficiency with 99.87% of mineralization in approximately 2 h of treatment. On the other hand, photoelectrocatalysis in $NaNO_3$ and NaCl promotes only 76 and 44% after 3 h of treatment, respectively.

The supporting electrolytes play important role in a photoelectrocatalytic process. In the ideal n-type semiconductor/electrolyte

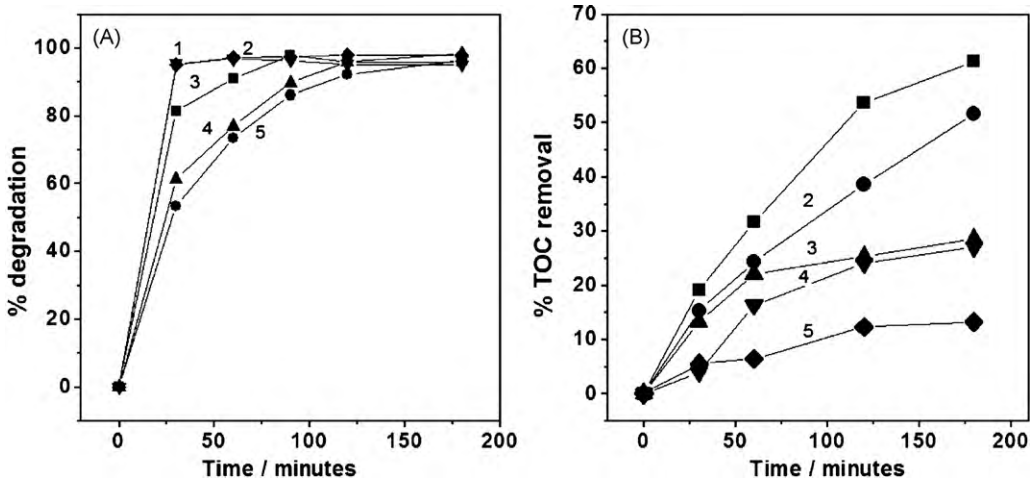

Fig. 7. Effect of initial concentration of aromatic amine ODAN on PEC degradation at bias potential 1.5 V (vs. Ag/AgCl), pH 6.0 and concentration of Na_2SO_4 0.1 mol L^{-1}, monitored by absorbance at 244 nm (A) and TOC removal (B), where amine concentration was: (1) 1.0×10^{-6}; (2) 5.0×10^{-6}; (3) 1.0×10^{-5}; (4) 5.0×10^{-5} and (5) 1.0×10^{-4} mol L^{-1}.

model upon bandgap illumination, the minority carrier (h^+) population is greatly enhanced, since the generated electrons are forcibly drawn to a conductor counter electrode. So, near the electrolyte/semiconductor interface, a potential barrier or band bending appears as a consequence of the electric field, which is intrinsic to the space charge region. The contact of a semiconductor with an electrolyte fortunately creates a junction that separates the carriers much like what happens at a metal/semiconductor contact [43–45]. In addition, the adsorption of this electrolyte can compete with water oxidation by h^+ on electrode surface, decreasing the hydroxyl radical formation, which is preponderantly responsible for the rapid degradation of pollutant, since h^+ has a shorter lifetime. So, although the supporting electrolyte helps the process of reducing band bending the competition between chloride ion and water for the positive photo-generated holes could decreases the process efficiency [17]. In addition, the photoelectrocatalysis conducted in nitrate is low efficiency, since part of the irradiation of $\lambda < 380$ nm is utilized on competitive photolytic reaction of NO_3^- by the overall reaction 3 [16]:

$$NO_3^- + H_2O + h\nu \rightarrow NO_2^{\bullet} + OH^{\bullet} + OH^- \quad (3)$$

Thus, Na_2SO_4 was chosen as best supporting electrolyte.

The effect Na_2SO_4 concentration was also evaluated testing the degradation of 5.0×10^{-6} mol L^{-1} of ODAN in 0.05; 0.1; 0.5 and 1.0 mol L^{-1} Na_2SO_4. Largest efficiency was obtained in 0.1 mol L^{-1} of Na_2SO_4, which promoted 100% of mineralization (TOC removal), while this value is reduced to 53% in 0.05 mol L^{-1}. Therefore, the concentration of 0.1 mol L^{-1} of Na_2SO_4 was adopted to optimize the method.

The effect of initial pH of solution 5.0×10^{-6} mol L^{-1} ODAN on photoelectrocatalytic oxidation at TiO_2 nanotube arrays electrode was investigated from 2 to 11. The results obtained during degradation (Fig. 9A) and TOC reduction were shown in Fig. 9B. The system is operating on degradation of ODAN on all pH values reaching approximately 100% of removal of signal. But, the largest percentages of ODAN mineralization are verified at pH 2, where smaller time is necessary to reach maximum efficiency of 100% removal. At basic conditions (pH 11) the efficiency is very poor. Since TiO_2 usually has an isoelectric point at a pH 5.7, it would seem that ODAN (or the intermediates photogenerated) are preferentially adsorbed when the TiO_2 surface is in protonated form leading to higher mineralization efficiencies at acidic medium. Thus pH values lower than 5 should be recommended as the optimal pH.

3.6. Comparison of nanotubular and nanoporous electrode performance on ODAN degradation

In order to test the superior performance of TiO_2 nanotubular arrays electrode in relation to nanoporous electrodes prepared by the method sol–gel, the degradation of ODAN was moni-

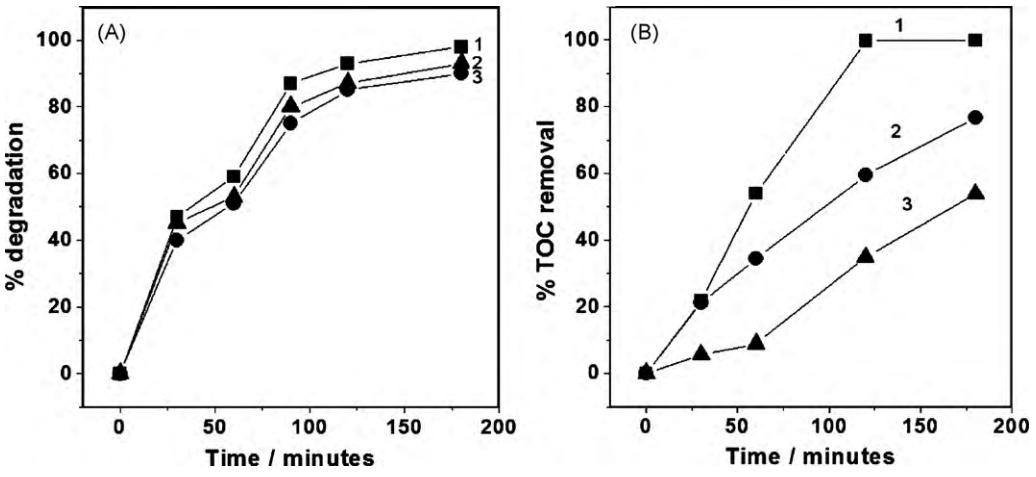

Fig. 8. PEC degradation of ODAN, monitored by absorbance at 244 nm (A) and TOC removal (B) as affected by type of support electrolyte (initial concentration of ODAN 5.0×10^{-6} mol L^{-1}, bias potential 1.5 V (vs. Ag/AgCl)), in: (1) Na_2SO_4; (2) $NaNO_3$ and (3) NaCl at 0.1 mol L^{-1} pH 2.0.

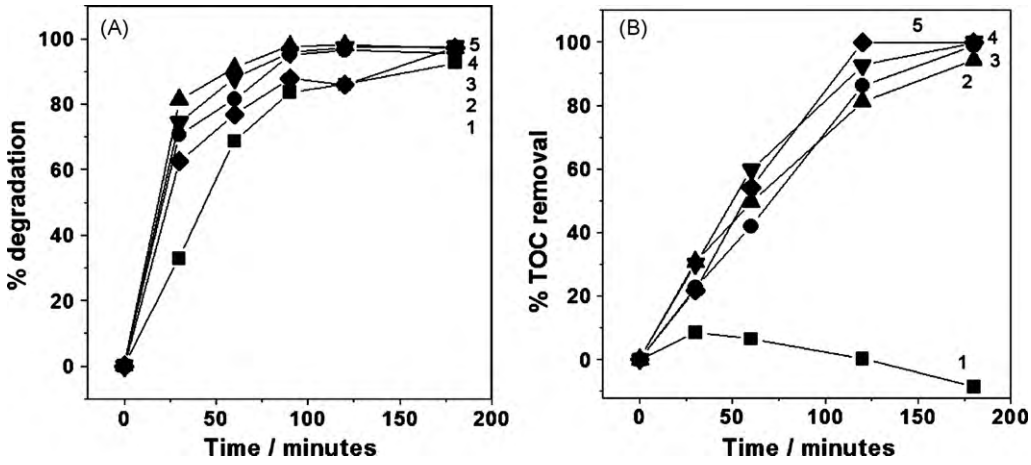

Fig. 9. PEC degradation of ODAN monitored by absorbance at 244 nm (A) and TOC removal (B) as affected by pH (initial concentration of ODAN 5.0×10^{-6} mol L^{-1}, bias potential 1.5 V (vs. Ag/AgCl)), Na_2SO_4 0.1 mol L^{-1} at pH values: (1) pH 11; (2) pH 9.0; (3) pH 7.0; (4) 5.0 and (5) pH 2.0.

tored using photolysis, PT (UV irradiation), photocatalysis, PC (UV irradiation + catalyst Ti/TiO_2) and photoelectrocatalysis, PEC (UV irradiation + Ti/TiO_2 + potential of 1.5 V) methods. Fig. 10 shows the percentage of mineralization (TOC removal) obtained during 180 min of treatment using the best conditions previously optimized: supporting electrolyte 0.1 mol L^{-1} Na_2SO_4, pH 2.0, applied potential of +1.5 V and ODAN concentration of 5.0×10^{-6} mol L^{-1}.

The PC and PT results indicates a mineralization lower than 50% of the initial solution and it is not dependent on the electrode material, confirming that the large surface area of the nanotubular array structure can enhance the efficiency of light energy conversion and maximize the number of photogenerated electron–hole pairs, but it is not the preponderant effect to promote degradation of amine. In addition, the results obtained for photolysis indicates that part of the amine is degraded only by UV irradiation. But, photoelectrocatalysis method have shown marked increases in the mineralization of ODAN, which promotes 100% of ODAN and offer a method for complete aromatic amine removal after 120 min of treatment. In addition, the comparison of the nanotubular electrode performance in relation to the nanoporous electrode for ODAN mineralization indicates a 50% increase in efficiency after only 2 h of PEC treatment.

These results confirm that the ordered nanotube arrays are very favorable for the transport of the photogenerated electrons in the TiO_2 film, which is very important in the PEC process. Irradiated by UV light, the applied positive bias to Ti/TiO_2 electrode can drive the photogenerated electrons in a vectorial channel to transport quickly to the counter electrode [46], which increases the lifetime of photogenerated holes and therefore dramatically improves the degradation rate of aromatic amines.

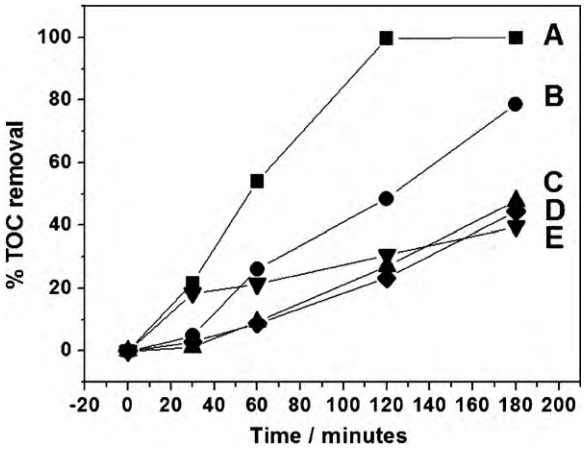

Fig. 10. PEC, PC and PT process of mineralization of aromatic amine ODAN where: (A) PEC—nanotubes; (B) PEC—nanoporous; (C) PC—nanotubes; (D) PC—nanoporous and (E) PT. Time = 180 min.

4. Conclusion

In conclusion, self-organized Ti/TiO_2 nanotubular array electrodes can be achieved by simple electrochemical anodization of Ti foil in NH_4F/glycerol water solution. The photocurrent on nanotube layers is remarkably improved in relation to that obtained on comparable nanoporous TiO_2 film obtained by sol gel process. The anatase form is priori in the highly ordered TiO_2 annealed at 450 °C and is more efficient in photoelectrocatalysis, because it improves the photoactivity. Both electrodes promote the complete degradation of the investigated aromatic amine ODAN after 120 min of phtooeletrocatalytic oxidation on potential of 1.5 V and UV irradiation. But, the ODAN mineralization is about 50% more efficient on the nanotube electrode. The favorable electron transport on nanotubular arrays is further supported by the enhanced degradation rate compared with a Ti/TiO_2 particulate film during the PEC aromatic amine. The method achieves a much better performance for treatment of water and wastewater contaminated by aromatic amines.

Acknowledgments

The authors acknowledge the financial support provided by the Brazilian funding agency FAPESP process 2007/07313-3; LME-LNLS, Campinas, Brazil, for the use of FEG-SEM.

References

[1] A. Fujishima, T.N. Rao, D.A. Tryk, Electrochim. Acta 45 (2000) 4683–4690.
[2] M. Gratzel, Nature 414 (2001) 338–344.
[3] O.K. Tan, W. Cao, Y. Hu, W. Zhu, Ceram. Int. 30 (2004) 1127–1133.
[4] I.M. Arabatzis, S. Antonaraki, T. Stergiopoulos, A. Hiskia, E. Papaconstantinou, M.C. Bernard, P. Falaras, J. Photochem. Photobiol. A: Chem. 149 (2002) 237–245.
[5] G.R. Reddy, A. Lavanya, C. Anjaneyulu, Bull. Electrochem. 20 (2004) 337–341.
[6] S. Hore, E. Palomares, H. Smit, N.J. Bakker, P. Comte, P. Liska, K.R. Thampi, J.M. Kroon, A. Hinsch, J.R. Durrant, J. Mater. Chem. 15 (2005) 412–418.
[7] P. Hoyer, Langmuir 12 (1996) 1411–1413.
[8] B.B. Lakshmi, P.K. Dorhout, C.R. Martin, Chem. Mater. 9 (1997) 857–862.
[9] H. Imai, Y. Takei, K. Shimizu, M. Matsuda, H. Hirashima, J. Mater. Chem. 9 (1999) 2971–2972.
[10] A. Michailowski, D. AlMawlwai, G.S. Cheng, M. Moskovits, Chem. Phys. Lett. 349 (2001) 1–5.

[11] J.H. Jung, H. Kobayashi, K.J.C. van Bommel, S. Shinkai, T. Shimizu, Chem. Mater. 14 (2002) 1445–1447.
[12] S. Kobayashi, N. Hamasaki, M. Suzuki, M. Kimura, H. Shirai, K. Hanabusa, J. Am. Chem. Soc. 124 (2002) 6550–6551.
[13] Z.R.R. Tian, J.A. Voigt, J. Liu, B. McKenzie, H.F. Xu, J. Am. Chem. Soc. 125 (2003) 12384–12385.
[14] T. Kasuga, M. Hiramatsu, A. Hoson, T. Sekino, K. Niihara, Langmuir 14 (1998) 3160–3163.
[15] K. Rajeshwar, M.E. Osugi, W. Chanmanee, C.R. Chenthamarakshan, M.V.B. Zanoni, P. Kajitvichyanukuld, R. Krishnan-Ayer, J. Photochem. Photobiol. C: Photochem. 9 (2008) 171–192.
[16] M.V.B. Zanoni, J.J. Sene, M.A. Anderson, J. Photochem. Photobiol. A: Chem. 157 (2003) 55–63.
[17] P.A. Carneiro, M.E. Osugi, J.J. Sene, M.A. Anderson, M.V.B. Zanoni, Electrochim. Acta 49 (2004) 3807–3820.
[18] M.E. Osugi, G.A. Umbuzeiro, M.A. Anderson, M.V.B. Zanoni, Electrochim. Acta 50 (2005) 5261–5269.
[19] M.E. Osugi, G.A. Umbuzeiro, F.J. de Castro, M.V.B. Zanoni, J. Hazard. Mater. B137 (2006) 871–877.
[20] S. Bauer, S. Kleber, P. Schmuki, Electrochem. Commun. 8 (2006) 1321–1325.
[21] H. Tsuchiya, J.M. Macak, A. Ghicov, P. Schmuki, Small 2 (2006) 888–891.
[22] S.P. Albu, A. Ghicov, J.M. Macak, P. Schmuki, Phys. Status Solidi RRL 1 (2007) R65–R67.
[23] J.M. Macak, S.P. Albu, P. Schmuki, Phys. Status Solidi RRL 1 (2007) 181–183.
[24] G.K. Mor, O.K. Varghese, M. Paulose, N. Mukherjee, C.A. Grimes, J. Mater. Res. 18 (2003) 2588.
[25] K. Shankar, G.K. Mor, H.E. Prakasam, O.K. Varghese, C.A. Grimes, Langmuir 23 (2007) 12445–12449.
[26] J.J. Sene, W.A. Zeltner, M.A. Anderson, J. Phys. Chem. B 107 (2003) 1597–1603.
[27] T. Niu, Y.Q. Cu, Mater. Res. Bull. 45 (2010) 536–541.
[28] R.A. May, H. Uchida, Thin Solid Films 518 (2010) 3169–3176.
[29] D. Gong, C.A. Grimes, O.K. Varghese, J. Mater. Res. 16 (2001) 3331–3334.
[30] Q. Cai, M. Paulose, O.K. Varghese, C.A. Grimes, J. Mater. Res. 20 (2005) 230–236.
[31] K. Shankar, G.K. Mor, A. Fitzgerald, C.A. Grimes, J. Phys. Chem. C 111 (2007) 21–26.
[32] M. Paulose, K. Shankar, S. Yoriya, H.E. Prakasam, O.K. Varghese, G.K. Mor, T.A. Latempa, A. Fitzgerald, C.A. Grimes, J. Phys. Chem. B 110 (2006) 16179–16184.
[33] K. Shankar, G.K. Mor, H.E. Prakasam, S. Yoriya, M. Paulose, O.K. Varghese, C.A. Grimes, Nanotechnology 18 (2007) 065707/1–065707/11.
[34] J.M. Macak, H. Tsuchiya, L. Taveira, S. Aldabergerova, P. Schmuki, Angew. Chem. Int. Ed. 44 (2005) 7463–7465.
[35] T. Tsubota, A. Ono, N. Murakami, T. Ohnoa, Appl. Catal. B: Environ. 91 (2009) 533–538.
[36] J. Lin, R. Zong, M. Zhou, Y. Zhu, Appl. Catal. B: Environ. 89 (2009) 425–431.
[37] R. Beranek, H. Hildebrand, P. Schumki, Electrochem. Solid-State Lett. 6 (2003) B12–B14.
[38] J.M. Macak, K. Sirotna, P. Schmuki, Electrochim. Acta 50 (2005) 3679–3684.
[39] J.M. Macak, H. Tsuchiya, P. Schmuki, Angew. Chem. Int. Ed. 44 (2005) 2100–2102.
[40] J. Van de Lagemaat, M. Plakman, D. Vanmaekelbergh, J. Kelly, J. Appl. Phys. Lett. 69 (1996) 2246–2248.
[41] J.P.H. Sukamto, W.H. Smyrl, C.S. Mcmillan, M.R.J. Kozlowski, Electrochem. Soc. 38 (1992) 15–27.
[42] B. Neppolian, H.C. Choi, S. Sakthivel, B. Arabindoo, V. Murugesan, J. Hazard. Mater. B89 (2002) 303–317.
[43] W.Z. Tang, Z. Zhang, H. An, M.O. Quintana, D.F. Torres, Environ. Technol. 18 (1997) 1–12.
[44] H.O. Finklea, Semiconductor Electrodes, Elsevier, New York, 1988.
[45] K. Rajeshwar, I. Jorge, Environmental Electrochemistry, first ed., Academic Press, INC, California, 1997.
[46] G.K. Mor, O.K. Varghese, M. Paulose, K. Shankar, C.A. Grimes, Sol. Energy Mater. Sol. Cells 90 (2006) 2011–2075.